

---

## ARTICLE

---

### Raman Studies of Advanced Gas-Cooled Reactor Simulated Spent Nuclear Fuels

R.J. Wilbraham<sup>a</sup>, N. Rauff-Nisthar<sup>a</sup>, C. Boxall<sup>a\*</sup>, E.A. Howett<sup>a</sup>, D.I. Hambley<sup>b</sup>, Z. Hiezl<sup>c</sup>, W.E. Lee<sup>c</sup> and C. Padovani<sup>d</sup>

<sup>a</sup>Engineering Department, Lancaster University, Lancaster, LA1 4YW, UK; <sup>b</sup>Spent Fuel Management and Disposal, UK National Nuclear Laboratory (NNL), Central Laboratory, Sellafield CA20 1PG, UK; <sup>c</sup>Department of Materials, Imperial College, London SW7 2AZ, UK; <sup>d</sup>Radioactive Waste Management Limited, Harwell OX11 0RH, UK

Analysis of advanced gas-cooled reactor (AGR) simulated used nuclear fuels (SIMFuels) has been carried out using micro-Raman spectroscopy in order to understand the effect lanthanide species (e.g. Nd, Y, Ce), representative of fission products generated during fuel burnup, have on the structure of the UO<sub>2</sub> matrix in spent AGR fuel. Results show a decrease in perfect fluorite character with increasing burnup as well as the development of a broad lattice distortion peak between 500 and 650 cm<sup>-1</sup>. Peak analysis of this broad band reveals it comprised of three overlapping peaks at 534 cm<sup>-1</sup>, 574 cm<sup>-1</sup> and 624 cm<sup>-1</sup>. The peak at 534 cm<sup>-1</sup> has been examined and is suggested to be due to a local phonon mode associated with oxygen-vacancy-induced lattice distortion as a result of lanthanide 3+ ion incorporation into the UO<sub>2</sub> bulk matrix.

**Keywords:** Raman Microscopy; Uranium Dioxide; SIMFuel; Advanced Gas Reactor;

#### 1. Introduction

In the UK, the vast proportion of spent nuclear fuel (SNF) is from indigenous advanced gas-cooled reactors (AGR). AGR reactors have several unique characteristics. First, the UO<sub>2</sub> fuel is annular in shape and clad in stainless steel rather than zircalloy. Secondly, fuel assemblies are moderated via a graphite core and coolant exit temperatures are almost twice that of LWR reactors. With the shift in UK energy strategy towards geological disposal rather than reprocessing, understanding of the durability of AGR fuels under disposal conditions relevant to UK geology has become a pressing research area [1]. However, handling of highly radioactive AGR spent nuclear fuel presents many barriers to the detailed scientific study of such parameters. Thus, in 2011 a consortium of UK academic and industrial institutions was set up to create the first UK specific simulated spent AGR nuclear fuels (SIMFuel), providing low and high burn-up fuel surrogates that can be studied in low activity laboratories without the complication of an intense radiation field. A detailed microstructural analysis of these SIMFuel samples, including SEM-EDX and XRD measurements, has been previously reported [2,3]. SIMFuel has been found to be inhomogeneous, containing a bulk UO<sub>2</sub> matrix, noble metal particulates ( $\epsilon$ -phase particles) and perovskite precipitates (or 'grey phase').

Here we report a vibrational analysis of these materials using micro-Raman spectroscopy, with a focus on the effect lanthanide species (Nd, Y and Ce), representative of fission products generated during fuel burnup, have on the vibrational spectrum of the bulk UO<sub>2</sub> fuel matrix. Micro-Raman allows localized chemical state interrogation of the bulk UO<sub>2</sub> matrix in SIMFuel not possible with either SEM-EDX or powder XRD. Such data is particularly useful in predicting the electrochemical corrosion behaviour of nuclear fuel, for example the degree of initial material oxidation [4] and the inhibiting effect lanthanide fission products may have on fuel dissolution [5]. The use of micro-Raman for the analysis of stoichiometric UO<sub>2</sub> [6], hyperstoichiometric UO<sub>2</sub> [4] and doped UO<sub>2</sub> materials [5] has seen much interest in the last 10 years. Through careful peak analysis, vibrational contributions in the Raman shift region 500-700 cm<sup>-1</sup> have been assigned to oxygen vacancies (resulting from Ln<sup>3+</sup> incorporation) and oxygen interstitials (and clusters of interstitials), the latter allowing determination of the oxygen to metal ratio (i.e. the degree of hyperstoichiometry).

#### 2. Experimental

##### 2.1. Materials

Depleted UO<sub>2</sub> powder manufactured from UF<sub>6</sub> was provided by National Nuclear Laboratory (Springfields, UK). All other chemicals were of AnalaR grade or better and supplied by either Alfa Aesar (Heysham, Lancashire,

---

\*Corresponding author. Email: [c.boxall@lancaster.ac.uk](mailto:c.boxall@lancaster.ac.uk)

UK) or Sigma Aldrich (Gillingham, Dorset, UK).

## 2.2. Preparation of AGR SIMFuel Samples

A detailed description of the preparation of undoped  $\text{UO}_2$ , 25 GWd/tU and 43 GWd/tU SIMFuel samples has been previously described elsewhere [2,3]. However, for the reader's convenience we briefly summarise the preparation process below:

Spent AGR fuel compositions for 25 GWd/t U and 43 GWd/t U simulated burnup and after 100 years cooling, time were first calculated using FISPIN 10.0.1 code [3]. Due to their miscibility in urania and close periodicity Pu, Am, Cm, Sm, Pr, Pm and Np were replaced by additional  $\text{UO}_2$ , with the final simulated material composition shown in **Table 1**.

Table 1. FISPIN calculated AGR SIMFuel composition used to create the samples described here after 100 years cooling time for both 25 and 43 GWd/t U burnup.

SIMFuel Composition (at%)	25 GWd/t U Burnup	43 GWd/t U Burnup
$\text{UO}_2$	95.705	92.748
$\text{Nd}_2\text{O}_3$	0.761	1.284
$\text{ZrO}_2$	0.793	1.276
$\text{MoO}_3$	0.614	1.027
$\text{RuO}_2$	0.512	0.892
$\text{BaCO}_3$	0.328	0.576
$\text{CeO}_2$	0.297	0.499
$\text{PdO}$	0.195	0.425
$\text{Rh}_2\text{O}_3$	0.080	0.115
$\text{La}_2\text{O}_3$	0.156	0.256
$\text{SrO}$	0.081	0.126
$\text{Y}_2\text{O}_3$	0.095	0.149
$\text{Cs}_2\text{CO}_3$	0.311	0.495
$\text{TeO}_2$	0.073	0.130

A 60 g blend of each composition was then generated based on Table 1. The blend was ball milled overnight using a  $\text{ZrO}_2$  milling medium. After repeated sieving, powders were pre-compacted into granulates at a pressure of 75 MPa. Next 0.2 wt. % zinc stearate was added as a lubricant and slowly mixed in using a rotary mixer. The granulates were then pressed into green pellets in a uniaxial press by applying a pressure of 400 MPa. Pellets were then sintered in a refractory metal furnace at a heating rate of 5 °C/min to 300°C, and then 15°C/min to 1730°C under 99.5 at. %  $\text{H}_2$  and 0.5 at. %  $\text{CO}_2$  atmosphere, for a total sintering time of 300 minutes. After cooling, the finished pellets were cut into slices ranging from ~1–3 mm thick using a precision cut-off machine with diamond cut-off wheel and surface polished using 600 grit SiC paper.

## 2.3. Raman Analysis of AGR SIMFuel Samples

$\mu$ -Raman Spectra were acquired using a Voyage confocal Raman microscope system (B&W Tek, Newark, USA). All spectra were acquired at an

excitation wavelength of 785 nm. Before analysis, laser power was adjusted to < 5mW using neutral density filters in order to avoid any thermal oxidation of  $\text{UO}_2$  to  $\text{U}_3\text{O}_8$  [5]. Typical analysis of each sample involved focusing the laser beam on the sample through a 50x objective lens before taking a spectra using an integration time of 40000 milliseconds over a wavenumber range from 190 to 3000  $\text{cm}^{-1}$ . For the analysis of each sample, an average of 20 spectra were recorded at different locations across the sample, being careful to avoid any large noble metal ( $\epsilon$ -phase) particles or  $\text{BaZrO}_3$  phases [7,8], in order to account for natural variations in oxygen to metal ratio in the SIMFuel bulk  $\text{UO}_2$  matrix [9].

## 3. Results and Discussion

$\mu$ Raman spectra of undoped  $\text{UO}_2$ , 25 GWd/t U and 43 GWd/t U AGR SIMFuel samples over the wavenumber range 300 to 800  $\text{cm}^{-1}$  are shown in **Figure 1**.

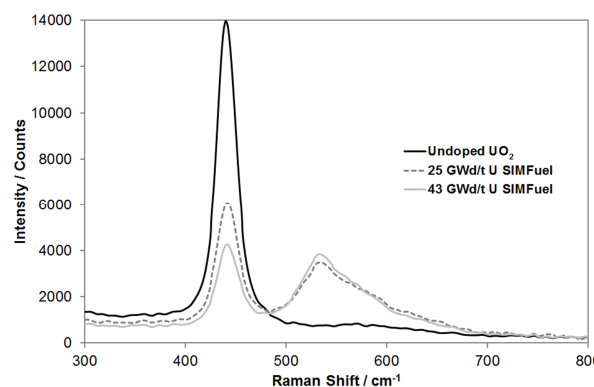


Figure 1.  $\mu$ Raman spectra recorded from undoped  $\text{UO}_2$ , 25 GWd/t U SIMFuel and 43 GWd/t U SIMFuel pellets.

Considering first the  $\mu$ -Raman spectrum of the undoped uranium dioxide sample in Figure 1, group theory predicts that a perfect fluorite structure would be expected to give a triply degenerate Raman active mode ( $T_{2g}$ ) [10], frequently defined as the fundamental U-O symmetric stretching mode [5]. This intense vibration typically appears at ~445  $\text{cm}^{-1}$  and in our sample is very close to this value at 442  $\text{cm}^{-1}$ .

Turning now to the two SIMFuel samples, it can be seen from Figure 1 that there is a clear decrease in intensity of the U-O fundamental stretch with increasing simulated burnup. Such a marked decrease in this peak is indicative of movement away from a perfect fluorite lattice structure, either via non-stoichiometry or introduction of dopant defects [4,5]. Furthermore a new broad band is observed between ~500 and 650  $\text{cm}^{-1}$  and has been previously ascribed by He *et al.* as due to lattice distortions resulting from fission product doping [9].

In order to deconvolute the various component peaks that comprise the broad band between 500 and 650  $\text{cm}^{-1}$  an initial linear baseline correction was carried out over the range 370-750  $\text{cm}^{-1}$ , followed by peak wavenumber

identification based on the downward zero-crossings in the smoothed first derivative of the spectrum. Having determined the main contributors, a multiple unconstrained Lorentzian fit was conducted using an iterative least-squares fit at the obtained wavenumber values. An example of this analysis for the 25 GWd/tU simulated burnup SIMFuel sample is shown in **Figure 2**.

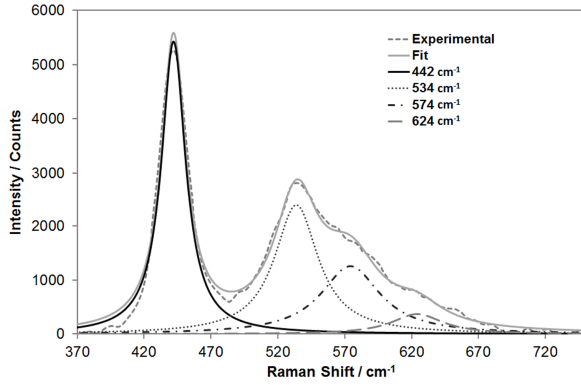


Figure 2. Example Lorentzian profile analysis of 25 GWd/t U SIMFuel over the range of 370-750  $\text{cm}^{-1}$ .

For both SIMFuel samples, three overlapping peaks are identified as contributing to the broad band between 500 and 650  $\text{cm}^{-1}$ : 534  $\text{cm}^{-1}$ , 574  $\text{cm}^{-1}$  and 624  $\text{cm}^{-1}$ . Here we focus on the origin of the 534  $\text{cm}^{-1}$  peak of these samples.

The 534  $\text{cm}^{-1}$  peak has previously been assigned in un-doped  $\text{UO}_2$  to various different effects. First, Livneh and Sterer [11] report that a degenerate phonon band with high density of states can be resolved at 515  $\text{cm}^{-1}$ . However, such a feature only appears in  $\text{UO}_2$  above ambient pressure and at laser excitation wavelengths different to that used here.

Under ambient pressure, both Guimbretière *et al.* [12] and, more recently Onofri *et al.* [13], report the appearance of a peak at 540  $\text{cm}^{-1}$  in  $\text{UO}_2$  irradiated with He and Kr respectively. Guimbretière *et al.* [12] suggest that this peak could be  $\text{UO}_{2-x}$  hypostoichiometry defects, created as an accompaniment to  $\text{UO}_{2+x}$  hyperstoichiometry defects (i.e. interstitial oxygens entering the lattice).

As the samples of Figure 1 have not been irradiated or ion implanted, the large increase in the 534  $\text{cm}^{-1}$  band in our SIMFuel samples must therefore be dopant related. Comparison with Raman spectra of CANDU/LWR SIMFuel samples by He *et al.* [9], reveals a similar peak at 540  $\text{cm}^{-1}$ . This feature is attributed by the authors to (Ba,Sr)ZrO<sub>3</sub> perovskite precipitates within the sample. However, as noted in the experimental section, in this study care was taken to avoid noble metal ( $\epsilon$ -phase) particles or BaZrO<sub>3</sub> phases within the SIMFuel materials, a discrimination not employed by He *et al.*. Thus, we are confident that spectra are only being acquired of the bulk  $\text{UO}_2$  matrix and the dissolved dopant oxides contained therein and we disagree with this previous assessment that the 534  $\text{cm}^{-1}$  band is related to (Ba,Sr)ZrO<sub>3</sub> perovskite precipitates.

In support of the above assessment, alternative assignments for the 534  $\text{cm}^{-1}$  peak have recently been provided by, Lee *et al.* [14], Razdan and Shoesmith [5], Desgranges *et al.* [15] and Talip *et al.* [16], through Raman measurements of Gd-doped  $\text{UO}_2$ , Dy-doped  $\text{UO}_2$ , Nd-doped  $\text{UO}_2$  and La-doped  $\text{UO}_2$  respectively. In all cases the 530-540  $\text{cm}^{-1}$  peak was found to increase with increasing lanthanide content. Furthermore, based on defect models by Park and Olander of Gd, Eu [17] and Nd [18] and Raman studies of lanthanide (III) doped  $\text{UO}_2$  [5,14-16], there is general agreement that the peak at 530-540  $\text{cm}^{-1}$  is a local phonon mode associated with oxygen-vacancy-induced lattice distortion, said oxygen vacancies created as charge compensation for the incorporation of the 3+ lanthanide dopant into the bulk  $\text{UO}_2$  matrix.

In order to assess differences in peak intensity between the two SIMFuels, the integrated peak area of the deconvoluted 534  $\text{cm}^{-1}$  peak for both the 25 GWd/t U and 43 GWd/t U was calculated and compared, with the results shown in **Figure 3**.

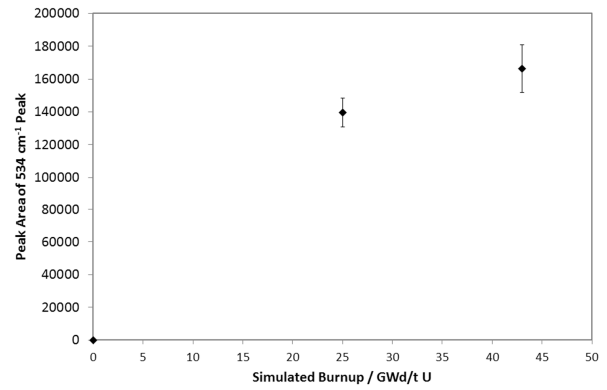


Figure 3. 534  $\text{cm}^{-1}$  peak area as a function of simulated burnup.

Figure 3, shows a significant increase in the 534  $\text{cm}^{-1}$  peak with increasing burnup. From Table 1 it can be seen that the primary dissolved lanthanide oxide dopant is neodymium (0.761 at. % and 1.284 at. % in the 25 and 43 GWd/t U SIMFuel samples respectively), with much lower amounts of lanthanum also present (0.156 at. % and 0.256 at. % respectively). There may also be some cerium dissolved in the matrix as well, although it is difficult to estimate how much, as some partitions into (Ba,Sr)ZrO<sub>3</sub> phases [2,3]. Hence, as our measurements are only taken of areas comprised of bulk  $\text{UO}_2$  containing dissolved dopant oxides, the increase in the 534  $\text{cm}^{-1}$  peak area with burnup in the SIMFuel samples of Figure 3 can be predominantly attributed to the formation of oxygen vacancies formed as a result of Nd and La doping. Finally, based on the calculations of Park [18], such oxygen vacancies may be found in the form of dopant-vacancy clusters, in the case of neodymium: (5U: V: 2Nd). Thus, Raman analysis of these materials suggests that, as previously proposed for LWR SIMFuel materials [5,8,9], lanthanide fission products in AGR SIMFuel are dispersed throughout the

UO<sub>2</sub> matrix as a solid solution of dopant-vacancy clusters,

### 3. Conclusion

Analysis of the bulk matrix of simulated spent advanced gas-cooled reactor nuclear fuel has been carried out using micro-Raman spectroscopy. Results show a decrease in perfect fluorite character with increasing burnup as well as the development of a broad lattice distortion peak between 500 and 650 cm<sup>-1</sup>. Peak analysis of this broad band reveals in it comprised of three overlapping peaks at 534 cm<sup>-1</sup>, 574 cm<sup>-1</sup> and 624 cm<sup>-1</sup>. The peak at 534 cm<sup>-1</sup> has been examined and is suggested to be due to a local phonon mode associated with oxygen-vacancy-induced lattice distortion as a result of lanthanide 3+ ion incorporation into the UO<sub>2</sub> bulk matrix, rather than the presence of a (Ba,Sr)ZrO<sub>3</sub> perovskite as previously described in Raman analysis of CANDU/LWR SIMFuels. As such, and as has been previously proposed for LWR SIMFuels, lanthanide fission products in AGR SIMFuel are dispersed throughout the UO<sub>2</sub> matrix as a solid solution of dopant-vacancy clusters.

### Acknowledgements

RJW and CB are supported by The Lloyd's Register Foundation (LRF). The Lloyd's Register Foundation supports the advancement of engineering-related education, and funds research and development that enhances safety of life at sea, on land and in the air.

### References

- [1] Department of Energy and Climate Change, Implementing geological disposal: A Framework for the long-term management of higher activity radioactive waste. URN 14D/235, UK Government, (2014), 1-54.
- [2] Z. Hiezl, D.I. Hambley, C. Padovani and W.E. Lee, Processing and microstructural characterization of a UO<sub>2</sub>-based ceramic for disposal studies on spent AGR fuel, *J. Nucl. Mat.* 456 (2015), pp.74-84.
- [3] Z. Hiezl, Processing and microstructural characterization of UO<sub>2</sub>-based simulated spent nuclear fuel ceramics for the UK's advanced gas-cooled reactors, Thesis, Imperial College London, (2015) pp.1-260.
- [4] H. He and D.W. Shoesmith, Raman spectroscopic studies of defect structures and phase transition in hyper-stoichiometric UO<sub>2+x</sub>, *Phys. Chem. Chem. Phys.* 12 (2010), pp. 8108-8117.
- [5] M. Razdan and D.W. Shoesmith, Influence of trivalent-dopants on the structural and electrochemical properties of uranium dioxide (UO<sub>2</sub>), *J. Electrochem. Soc.* 161 (2014), pp. H105-H113.
- [6] J. Lv, G. Li, S. Guo, and Y. Shi, Raman scattering from phonons and electronic excitations in UO<sub>2</sub> with different oxygen isotopes, *J. Raman Spectrosc.* 47 (2015), pp. 345-349.
- [7] J.I. Bramman, R.M. Sharpe, D. Thom, and G. Yates, Metallic fission-product inclusions in irradiated oxide fuels, *J. Nucl. Mater.* 25 (1968) pp. 201-215.
- [8] P.G. Lucata, R.A. Verral, H.J. Matzke, and B.J. Palmer, Microstructural features of SIMFUEL - simulated high-burnup UO<sub>2</sub>-based nuclear fuel, *J. Nucl. Mater.* 178 (1991), pp. 48-60.
- [9] H. He, P.G. Keech, M.E. Broczkowski, J.J. Noël, and D.W. Shoesmith, Characterization of the influence of fission product doping on the anodic reactivity of uranium dioxide, *Can. J. Chem.* 85 (2007), pp. 702-713.
- [10] G.C. Allen, Characterisation of uranium oxides by micro-Raman, *J. Nucl. Mater.* 144 (1987), pp. 17-19.
- [11] T. Livneh and E. Sterer, Effect of pressure on the resonant multiphonon Raman scattering in UO<sub>2</sub>, *Phys. Rev. B: Condens. Matter.* 73 (2006), pp. 085118.
- [12] G. Guimbretière, L. Desgranges, A. Canizares, G. Carlot, R. Carabello, C. Jégou, F. Duval, N. Raimboux, M.R. Ammar, and P. Simon, Determination of in-depth damaged profile by Raman line scan in a pre-cut He<sup>2+</sup> irradiated UO<sub>2</sub>, *Appl. Phys. Lett.* 100 (2012), pp. 251914-1-251914-4.
- [13] C. Onofri, C. Sabathier, H. Palancher, G. Carlot, S. Miro, Y. Serruys, L. Desgranges, and M. Legros, Evolution of extended defects in polycrystalline UO<sub>2</sub> under heavy ion irradiation: Combined TEM, XRD and Raman study, *Nucl. Instrum. Methods Phys. Res., Sect. B* 374 (2016), pp. 51-57.
- [14] J. Lee, J. Kim, Y.-S. Youn, N. Liu, J.-G. Kim, Y.-K. Ha, D.W. Shoesmith, and J.-Y. Kim, Raman study on structure of U<sub>1-y</sub>Gd<sub>y</sub>O<sub>2-x</sub> (y=0.005,0.01, 0.03, 0.05 and 0.1) solid solutions, *J. Nucl. Mater.* 486 (2017), pp. 216-221.
- [15] L. Desgranges, Y. Pontillon, P. Matheron, M. Marcet, P. Simon, G. Guimbretière, and F. Porcher, Miscibility gap in the U-Nd-O phase diagram: A new approach of nuclear oxides in the environment?, *Inorg. Chem.* 51 (2012), pp. 9147-9149.
- [16] Z. Talip, T. Wiss, P.E. Raison, J. Paillier, D. Manara, J. Somers, and R.J.M. Konings, Raman and X-ray studies of uranium-lanthanum-mixed oxides before and after air oxidation, *J. Am. Ceram. Soc.* 98 (2015), pp. 2278-2285.
- [17] K. Park and D.R. Olander, Defect model for the oxygen potentials of gadolinium- and europium-doped urania, *J. Nucl. Mater.* 187 (1992), pp. 89-96.
- [18] K. Park, The oxygen potential of neodymia-doped urania based on a defect structure, *J. Nucl. Mater.* 209 (1994), pp. 259-262.